



## ARTICLE

# Natural vegetation biomass and the dimension of forest quality in tropical agricultural landscapes

Renato Miazaki de Toledo<sup>1</sup>  | Vania Regina Pivello<sup>1</sup> |  
 Michael Philip Perring<sup>2,3</sup>  | Luciano Martins Verdade<sup>4</sup>

<sup>1</sup>LEPaC, Departamento de Ecologia, Instituto de Biociências, Universidade de São Paulo, São Paulo, Brazil

<sup>2</sup>UK Centre for Ecology and Hydrology (UKCEH), Bangor, UK

<sup>3</sup>The UWA Institute of Agriculture, The University of Western Australia, Perth, Western Australia, Australia

<sup>4</sup>LE<sup>2</sup>AVe, Centro de Energia Nuclear na Agricultura, Universidade de São Paulo, São Paulo, Brazil

## Correspondence

Renato Miazaki de Toledo  
 Email: [rmt@usp.br](mailto:rmt@usp.br)

## Funding information

CNPq-Brazilian Council for Scientific and Technological Development, Grant/Award Number: 304559/2021; FAPESP-São Paulo Research Foundation, Grant/Award Numbers: 17/01304-4, 20/10238-8, 21/00044-4

**Handling Editor:** Xiangming Xiao

## Abstract

Forest cover has been a pivotal indicator of biological conservation and carrying capacity for wildlife in forest ecoregions. Such a relationship underpins policies focused on the extension of protected lands. Here, we estimate aboveground biomass (AGB) as a proxy for habitat quality in seminatural rural patches and provide a comparison with approaches that only consider forest cover. We hypothesize that recommendations for biological conservation in agricultural landscapes are substantially improved if habitat quality is also taken into account, and thus consider the possibility of forest quality being modulated by land-use amount, type, and age. We assessed AGB in a densely farmed Brazilian region using a straightforward approach designed to be affordable at large scales, focusing on two expanding and contrasting land uses: sugarcane, and eucalyptus plantations. At a detailed scale, we confirmed through field surveys and AGB estimation using 3D-multispectral imagery (i.e.,  $AGB = 0.842 \times \text{vegetation height}^{NDVI+1}$ ) that AGB variation could be predicted with forest degradation classes that are visually distinguishable with high-resolution images:  $9.33 \text{ t ha}^{-1}$  (90% predictive intervals [PI] = [3.23, 26.97]) in regenerating fields (RF),  $31.12 \text{ t ha}^{-1}$  (90% PI = [10.77, 89.90]) in pioneer woods (PW), and  $149.04 \text{ t ha}^{-1}$  (90% PI = [51.59, 430.58]) in dense forests (DF). Applying these values to land units sampled across the study region, we found an average land use of 88.5%, together with 11.5% of land set aside for conservation, which reduced AGB to less than 4.2% of its potential (averages of  $5.85 \text{ t ha}^{-1}$  in sugarcane-dominated areas and  $6.56 \text{ t ha}^{-1}$  in eucalyptus-dominated areas, with secondary forests averaging  $149.04 \text{ t ha}^{-1}$ ). This imbalance between forest cover and AGB resulted from forest quality decay, which was similarly severe among land-use types, ages, and extensions. Therefore, the shortage of trophic resources is likely more critical to wildlife than spatial limitations in vastly deforested tropical ecoregions, where AGB and carbon sinks can be more than doubled just by restoring forests in lands currently spared by agriculture.

## KEYWORDS

degradation monitoring, forest fragments, habitat indicator, Southeast Brazil, trophic resources

## INTRODUCTION

Critical deforestation rates in tropical regions have been related to agricultural expansion (Dudley & Alexander, 2017; Nobre et al., 2016), but growing evidence indicates that degradation in forest remnants caused by neighboring land uses has been as harmful as intentional deforestation (Barlow et al., 2016). These concerns have been addressed by international agreements such as the Kyoto Protocol, the New York Declaration, and the Paris Agreement (Sotirov et al., 2020), which formalize the international community's interest in changing land-use trajectories in favor of biodiversity and ecosystem services. Agriculture covers nearly 5 billion ha, or 38% of the global land surface, and Brazil is the fourth-largest country in terms of agricultural land extent (pasture and cropland), covering 278 million ha (FAO, 2020), representing 4.4% of the world's cultivated lands (Potapov et al., 2022). Fragmentation gradually accelerates the loss of tropical forests after the initial human settlements (Hansen et al., 2020) and regenerated forest patches in agriculture-dominated landscapes can be ephemeral, tending to be cleared again for new land uses, as is the case in the Brazilian Atlantic Forest (Piffer et al., 2022).

In such a context, area-based conservation indicators have been used as a pivotal heuristic criterion for conservation guidelines and land-use regulation. Such territorial reference for biodiversity is grounded in well established ecological knowledge (Pimm et al., 2018), such as the Equilibrium Theory of Island Biogeography (MacArthur & Wilson, 1967). Accordingly, conservation and restoration priorities usually involve quantifying habitat cover (e.g., Banks-Leite et al., 2014; Myers et al., 2000). For example, the Aichi target n.11 (UNEP, United Nations Environment Programme World Conservation Monitoring Centre, 2016) established 17% as the minimum extent of protected lands by 2020. Twelve years later, the Kunming-Montreal target n.3 increased the protection goal for 30% of terrestrial and aquatic areas by 2030, implying massive forest restoration (Rayden et al., 2023). Also, Wilson (2016) and Dinerstein et al. (2017) proposed designating 50% of the ecosystem surface for conservation: a “half Earth” protection. Such territorial goals have been supported by studies that have found that major biodiversity losses are prevented in landscapes of more than 40% of forest cover (Arroyo-Rodríguez et al., 2020; Vidal et al., 2019).

Environmental commitments based on the amount of land use can be monitored by increasingly accessible remote sensing approaches (e.g., Silva-Junior et al., 2021). However, besides the practical benefits and the solid theoretical basis around area-based conservation metrics it is reasonable to question to what extent the amount of natural surface is indicative of primary production,

biodiversity, wildlife carrying capacity, and so many ecosystem attributes assumed as highly correlated with natural surface cover. Such associations may be particularly uncertain in highly modified landscapes because fragments accounted as natural may be highly degraded by surrounding uses (Barlow et al., 2016). Even so, most policies are only focused on the amount of area and neglect other environmental conditions. For instance, the environmental legal framework adopted in Brazil includes offsetting alternatives based on area parity rather than conservation status (de Mello et al., 2021).

Conversely, plant biomass has proven to be the primary driver of changes in ecosystem processes rates in the course of succession (Lohbeck et al., 2015), as well as an effective indicator of species richness (Satdichanh et al., 2019) and ecosystem functioning (Lohbeck et al., 2015; Poorter et al., 2021). Therefore, quantifying tropical forest biomass rather than only measuring forest cover is a promising alternative for better assessing the availability of natural resources to wildlife and the ecological conditions for biological complexity and diversity. The benefits of natural biomass assessments are arguably more critical in well established agricultural regions, as significant biomass loss resulting from increasing forest degradation is expected several years after deforestation has ceased (see Silva-Junior, Aragão, et al., 2020). Scientific agencies are promoting the fast development of various solutions for nondestructive aboveground biomass (AGB) estimation including tropical forests (Almeida et al., 2019; Duncanson et al., 2019; Labrière et al., 2022). Also, the proliferation of very high-resolution remote sensing resources stimulated innovative approaches for assessing forest structure and tree biomass (Almeida et al., 2019; Bastin et al., 2018). However, assessing high-resolution biomass variation in large regions remains challenging (de Almeida et al., 2020).

For this study, we developed a straightforward approach to quantify seminatural AGB in a densely agricultural Brazilian region. For broader applicability of results, we focused on two expanding agricultural uses: intensively agricultural and annually harvested sugarcane crop fields, which contrasts with eucalyptus forestry, which typically grows for years of minor interventions before being harvested. We investigated seminatural AGB as a unifying indicator of natural resources available for wildlife that could ideally be monitored by conservation programs and land-use regulation in agricultural landscapes, grounding enhanced inferences on biodiversity and biocomplexity compared to forest cover mapping. Along with testing the proposed approach, we addressed two questions and their implications: (1) How coupled are forest cover and AGB in agricultural landscapes? (2) Is the forest quality modulated

by surrounding land-use age or type? We expected disproportionally high AGB losses to follow forest cover losses because of forest degradation, which could be intensified over time, as supported by Barlow et al. (2016) and Silva-Junior, Teodoro, et al. (2020). The effect of the agricultural matrices on the fragments within them is expected to reflect biotic and abiotic particularities of land-use types, as supported by Verdade et al. (2014), (2016), and Arroyo-Rodríguez et al. (2020). Last, based on our study case, we discuss the practical consequences of adopting seminatural AGB as a measure of habitat quality, focusing on how to move forward on the path to more sustainable rural landscapes.

## METHODS

### Study region

The center-south of São Paulo state, the focus of our study region, has been extensively and profoundly modified by mechanized agriculture in the last century and has become one of the largest well established agro-industrial regions in Brazil (Dias et al., 2016). More recently, agricultural consolidation has caused the decline of deforestation and cattle ranching, as well as the rise of crop fields and industrial forestry (MapBiomas, 2022; Toledo et al., 2018).

To maintain the natural similarity across the study region, we selected the region based on the gradient between the semideciduous Atlantic Forest and the Cerrado woodland, as spatialized by IBGE (2017), and we established the latitudinal range between 20 and 23° South, which corresponds to the southern limit of the core Cerrado domain and the northern limit of the Araucaria Moist Forests, respectively. This criterion resulted in a 680 km-wide and 420 km-long area, encompassing 260,464 km<sup>2</sup>, or 3.1% of Brazilian land (Figure 1a,b). According to IBGE (2017) 98.9% of our study region was formerly covered by forests, 48% of Atlantic forests, 30% of Cerrado forests, and 21% of forested transitions. Currently, 24.8% of our study region is covered by sugarcane (6.5 million ha, 69.4% of Brazilian sugarcane fields), 3.2% by monocultural forestry (0.8 million ha, 11.1% of Brazilian monocultural forestry), 23.8% by pastures, 28.9% by other crops, 10.6% by natural forests, 0.5% by natural grasslands, 2.7% by wetlands 3.4% by water reservoirs, and 2.2% by urban areas. These figures characterize a land occupation that is relatively unusual in Brazil but becoming more widespread under current economic pressures (Souza Jr Carlos et al., 2020).

### Study design

The methodological approach we developed to estimate forest biomass in agricultural landscapes consisted of two phases, described in detail in the next sections. In summary, the first phase quantifies AGB of natural and seminatural origin (hereafter referred to as AGB, which excludes cultivated plants but includes spontaneous stems of indigenous, exotic, and naturalized species) in 21 reference land units (Figure 1b–d). Then, within the same areas, vegetation cover was classified into three classes (Figure 1e). The most degraded class, referred to as “regenerating fields” (RF), is characterized by herb dominance; the intermediate class, referred to as “pioneer woods” (PW), is predominantly covered by shrubs and trees but tree cover is not continuous; and the least degraded class, named “dense forests” (DF), is characterized by continuous tree cover (i.e., emergent crowns >4 m in diameter). The second phase projected AGB density on a larger scale that covered the entire study region (Figure 1a). We used recent high-resolution images from the Google Earth repository to quantify the abundance of these degradation stages by employing the RF-PW-DF classification at coordinates positioned at random within 83 sampling land units (Figure 1f).

### Data collection for AGB estimation

Fieldwork was undertaken in two agricultural mosaics, one of them dominated by eucalyptus forestry and the other, 70 km to the north, dominated by sugarcane plantations. Nine reference land units (sensu Zonneveld, 1989) with 400 m diameter were positioned in the sugarcane-dominated area, and 12 under the eucalyptus-dominated area, so that their central coordinates were located within a natural/seminatural fragment, being at least 1 km distant. Vegetation plots of 40 × 40 m were established at these central coordinates.

Inside the vegetation plots, single-stemmed and multistemmed trees with a combined basal area greater than 7.0 cm<sup>2</sup> (equivalent to the standard dbh >3 cm) were identified and measured. The nomenclature followed the “Flora do Brasil 2020” database (<https://floradobrasil.jbrj.gov.br>), according to the APG IV system (APG, Angiosperm Phylogeny Group, 2016). Tree heights were recorded in the field using metric precision and a telescopic pole as a reference. Direct measurements were possible for trees up to 8 m in height. Tree heights exceeding 8 m were estimated by visual comparison; thus, precision gradually decreased with increasing tree height. To review the heights of emergent trees we used digital surface measurements captured by an unmanned aerial vehicle (UAV; described below), and all original

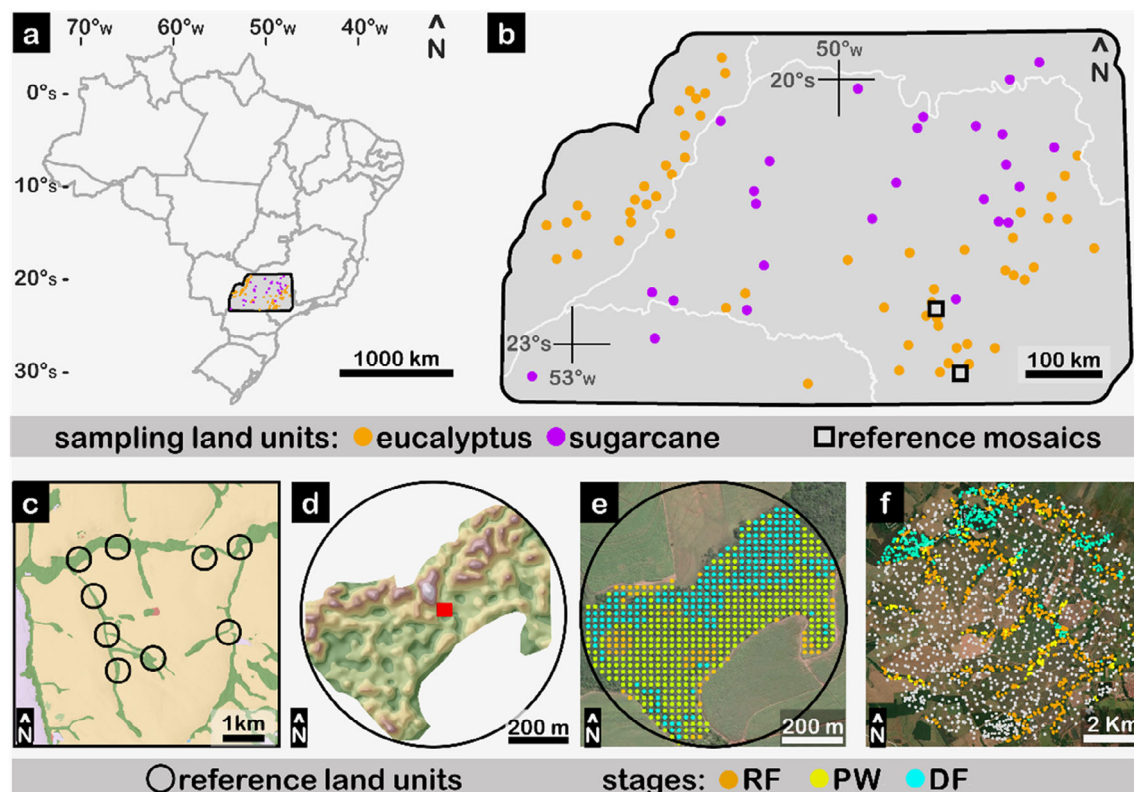


**FIGURE 1** (a) Geographical location of our study region, in Brazil; (b) study region and the position of reference mosaics as squares and sampling land units as circles; (c) sugarcane reference mosaic and respective reference land units; (d) aboveground biomass projection with 3D-NDVI data in a reference land unit and respective vegetation plot; (e) classification of vegetation degradation status in the same reference land unit; (f) relative abundance of the three degradation classes in a sampling land unit. DF, dense forests; PW, pioneer woodlands; RF, regenerating fields.

measurements were retained due to a lack of discrepancy (i.e., differences <25%). It should be noted that 68.2% of individuals were trees <8 m, and 91.3% had heights ≤10 m. In a perimeter up to 200 m around the vegetation plots we recorded the geographic position of 14 areas without trees and shrubs with dbh >3 cm, which served as a reference for open fields being spared from recent agricultural activities.

The single-winged UAV model XMOBOTS ARATOR 5B equipped with Sony RGB 5100 and X1M5 sensors was used to capture 3D multispectral data from all 21 reference land units, including the vegetation plots. Flights were conducted in February 2020. The 3D multispectral data were generated at a spatial resolution of 8 cm (including R, G, B, red-edge, near-infrared bands, and elevation) using the software Metashape 1.6.2. Additionally, a topographic survey collected ground elevation data in the image areas to enhance the accuracy of vegetation height measurements.

### Data collection for quantifying degradation classes

After collecting data for biomass estimates, we characterized and quantified the relative abundance of the

three degradation classes detectable by remote sensing. A 20 × 20 m grid was overlaid on the 21 reference land units for cell-by-cell classification of vegetation cover, using high-resolution RGB images available from Google Earth (i.e., Maxsar, from 2019 to 2020, at resolution <0.6 m). Our visual interpretation-based classification considered RF as having herbaceous cover >50% and shrub-tree cover <50%; PW comprised sites with herbaceous cover <50% and shrub-tree cover >50%, except when 100% canopy cover was achieved by emergent crowns wider than 4 m in diameter; this special case comprising continuous canopy cover of trees >4 m of diameter was taken as DF and made up the highest AGB condition.

The same RF-PW-DF classification was also used to sample land units scattered throughout the study region. First, the study regions' land cover map compiled from the MapBiomass platform (2022) (see Souza Jr Carlos et al., 2020) was rescaled to 1-km resolution, with pixel identity defined as the majority cover. We identified that sugarcane plantations were typically wider than 8 km, and eucalyptus plantations were typically wider than 3 km. These typical minimum dimensions were applied to the sampling land units as diameters, resulting in circular areas of 5027 ha for sugarcane and 707 ha for eucalyptus.



To optimize the sampling effort, random points were generated with an average density of two points per hectare within areas mapped as natural vegetation, and of 0.2 points  $\text{ha}^{-1}$  within areas mapped as “human land uses” (as in MapBiomass, 2022). Then, image interpretation was conducted within 61,616 circles of 20 m diameter randomly placed inside sampling land units randomly distributed within sugarcane and eucalyptus plantations across the study region. For each sample, we analyzed the most recent image available in the Google Earth repository, including data from different satellites, all with submeter resolution. Image source is provided for each one in Appendix S1: Table S2. Each circle was then visually classified according to the three degradation classes (RF, PW, and DF), or “human land uses” or “water body.” The relative density of each of these five land cover types was calculated at the sampling land-unit scale. In total, 26 sugarcane sampling land units and 57 eucalyptus sampling land units were needed to achieve sampling errors for average AGB density up to  $2 \text{ t ha}^{-1}$  at a 95% confidence level.

### AGB estimation using vegetation survey and multispectral 3D data

Each tree sampled in the field had its dry matter AGB estimated by an improved allometric equation for pantropical tree communities (Chave et al., 2014), using the diameter, height, and species identity:

$\text{AGB} = 0.063(\rho D^2 H)^{0.976}$ , where AGB = is the dry weight of aboveground biomass (in kilograms),  $\rho$  = specific density (in grams per cubic centimeter),  $D$  = diameter at breast height (in centimeters),  $H$  = height (in meters).

The specific wood density of each species was obtained from Chave et al. (2009) and Zanne et al. (2009). Species without references were associated with the average specific density of their respective genus. Likewise, individuals identified only at the genus or family levels were related to the mean specific density for the respective taxonomic level. We adopted the weighted average specific density of the respective community for individuals that could not be identified. Then, individual biomasses were summed by plot and expressed in tonne per hectare.

We combined the 35-plot level AGB measurements with the UAV dataset to select the linear model of greater parsimony and simplicity that combined normalized difference vegetation index (NDVI) and vegetation height as predictors of AGB through linear regression. The response variable was log-transformed to satisfy the homogeneity assumption. Central coordinates, average NDVI and average AGB measured inside all plots are

reported in Appendix S1: Table S1, which includes 21 plots of AGB >0 and 14 plots of AGB = 0.

The selected model was then applied to estimate biomass in the seminatural fragments inside the 21 reference land units with a spatial resolution of 20 m (6973 cells). The reason for using a 40-m resolution for modeling the relationship between field and UAV measurements, and then projecting AGB with UAV data in a 20-m resolution was that, on the one hand, our study required a spatial resolution of “few trees” to capture the heterogeneity we intended, including narrow corridors (i.e., 20-m), but, on the other hand, at that scale we observed a greater discrepancy between ground-level data and the “bird eye-view” of UAV data. That was because tree stems are entirely included or excluded as a standard field survey procedure, while remote sensing accounts for crowns partially projected over the plot. Therefore, we studied the relation between NDVI and tree height with a 40 m resolution to reduce unbalanced ratios of partial crowns from stems measured in the field. Thus, we used the same function found at the 40 m resolution in our 20 m projections, but with average values of NDVI and tree height taken at a 20 m resolution. We did not employ any interpolation technique.

### AGB assessment with degradation classes

We compared AGB estimate grids, generated with reference land units' 3D multispectral data, to degradation stage grids, generated by photointerpretation within reference land units, to assess the typical AGB patterns for each of the degradation classes. After employing variance analysis to check the relevance of taking into account AGB differences between sugarcane-dominated areas and eucalyptus-dominated, the average AGB values observed in RF, PW, and DF were applied to the sampling land units distributed throughout the study area, for which we had measured the densities of RF, PW, and DF.

### Spatial patterns and AGB drivers

To explore possible drivers of AGB observed in the sampling land units we considered that samples could be spatially nested by ecoregion (Dinerstein et al., 2017) and precolonial forest type (IBGE, 2017). Therefore, these two variables were accounted for as random variables in the linear mixed models (*nlme* package version 3.1-139, R-Core Team) that we used to test: (1) mapped forest cover, (2) the type of agricultural use, and (3) the age of current agricultural use (MapBiomass, 2022) as predictors of AGB (dataset provided in Appendix S1: Table S2).

The goodness-of-fit between models was compared with marginal and conditional  $R^2$  with MuMIn package version 1.43.6 (Nakagawa et al., 2017). In addition, spatial autocorrelation among AGB estimates was investigated with the global Moran's Index, calculated with the "spatial statistic tools" for ArcGIS 10.4 (ESRI, 2020).

## RESULTS

### Vegetation plots and degradation classes within the reference land units

Stem densities ranged from 56.3 to 1781.3 individuals/ha among plots (average = 737.5, SD = 517.16), which is consistent with a wide density range that comprises RF, and DF. The average AGB (i.e., seminatural woody AGB) at plot level was  $43.9 \text{ t ha}^{-1}$  (SE =  $\pm 6.7$ ), while the average NDVI in these 21 vegetation plots was 0.675 (SD = 0.256), and the average vegetation height was 7.8 m (SD = 4.4). Then, inside the 14 control samples that represented the complete absence of woody AGB, NDVI and average height were 0.384 and 1.1 m, respectively. The average AGB estimated in all regeneration fragments (seminatural fields and forests majorly composed of indigenous species) was  $59.3 \text{ t ha}^{-1}$ , between  $Q_{25} = 24.1 \text{ t ha}^{-1}$  and  $Q_{75} = 132.8 \text{ t ha}^{-1}$ . Most importantly, NDVI and vegetation height (H) are highly correlated with AGB (Spearman  $\rho = 0.800$  and Spearman  $\rho = 0.921$ , respectively). The best fitted model for AGB estimates was  $\text{AGB} = 0.842 \times H^{(\text{NDVI}+1)}$  (adjusted- $R^2 = 0.882$ ,  $F(1, 33) = 450.1$ ,  $p < 0.001$ ), with a significant effect of  $H^{(\text{NDVI}+1)}$  on AGB ( $\beta = 0.8423$ ,  $p < 0.001$ ) and a nonsignificant intercept of 0.942 ( $p = 0.702$ ). Frequency distributions of AGB, NDVI, tree height, and stem density for all plots are shown in Figure 2.

With the inspection of high-resolution images across the reference land units, we found that, within sugarcane-dominated areas, DF only covered 34.5% of the natural/seminatural fragments, while PW covered 43.8%, and RF covered 21.7%. Within eucalyptus-dominated areas, values of seminatural vegetation cover were 46.8% by DF, 43.8% by PW, and 5.3% by RF. Results corroborate the use of degradation classes as indicators of AGB, with a minor influence on agricultural land uses. The relationship between degradation stages and AGB was consistent in both agricultural matrices (Figure 3). The full model for AGB prediction considering the surrounding agricultural type and the degradation stage (i.e.,  $\text{AGB} \sim \text{agricultural type} + \text{degradation stage} \mid \text{reference land unit}$ ) showed a very high marginal determination coefficient (i.e.,  $R_m^2 = 0.676$ ), which was close to the conditional determinant

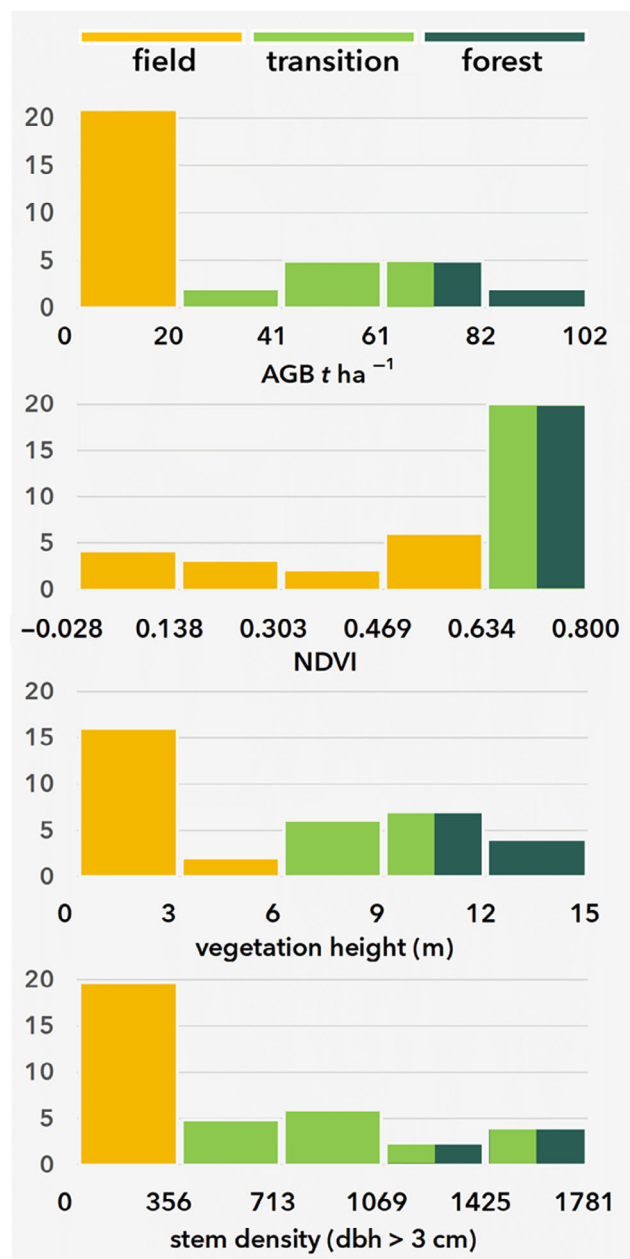


**FIGURE 2** Frequency of aboveground biomass (AGB), normalized difference vegetation index, vegetation height, and stem density among sample plots. The colors indicate the predominant type of vegetation in each category, or the two types that are similarly frequent.

coefficient (i.e.,  $R_c^2 = 0.704$ ). Although regenerating fragments surrounded by eucalyptus forestry showed slightly higher AGB than those surrounded by sugarcane, the significance of agricultural type as an AGB predictor was marginal ( $p = 0.0502$ ), with a nearly flat regression slope ( $\beta = 0.0810$  for eucalyptus-dominated landscapes). The simplified model that disregards agricultural type (i.e.,  $\text{AGB} \sim \text{degradation stage} \mid \text{reference land unit}$ ) resulted in a similar coefficient of determination ( $R_m^2 = 0.662$ ),

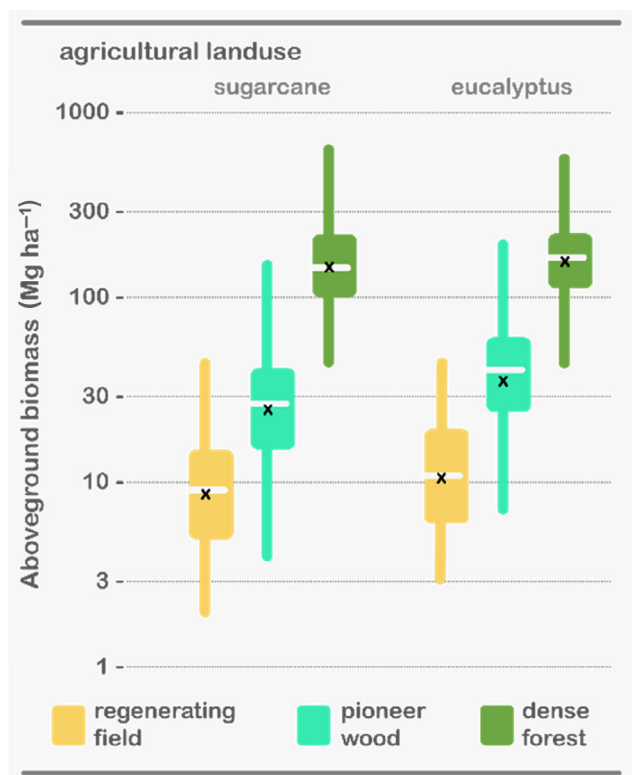


**FIGURE 3** Aboveground biomass (AGB) estimates based on vegetation height and normalized difference vegetation index as a function of forest regeneration classes that reflect degradation status (RF, PW, and DF) and agricultural land use (sugarcane plantations and eucalyptus forestry). Forest regeneration classes based on tree cover patterns explained 60.1% of AGB variation, while differences between land uses were minor ( $p = 0.0502$ ), only adding 0.8% to the model's determination coefficient. DF, dense forests; PW, pioneer woodlands; RF, regenerating fields.

and thus endorses degradation stage as an important predictor of AGB (i.e.,  $p < 0.0001$  in both models) in our analysis, the important predictor. Based on these results, our projections at the sampling land-unit scale considered AGB to have a mean of  $149.04 \text{ t ha}^{-1}$  (with 90% predictive intervals [PI] of [51.59, 430.58]) for the stage DF, of  $31.12 \text{ t ha}^{-1}$  (90% PI = [10.77, 89.90]) for the stage PW, and of  $9.33 \text{ t ha}^{-1}$  (90% PI = [3.23, 26.97]) for the stage RF. Based on these results, our following projections at the sampling land-unit scale considered AGB predictions of  $149.04 \text{ t ha}^{-1}$  (90% PI = [51.59, 430.58]) for the stage DF, of  $31.12 \text{ t ha}^{-1}$  (90% PI = [10.77, 89.90]) for the stage PW, and of  $9.33 \text{ t ha}^{-1}$  (90% PI = [3.23, 26.97]) for the stage RF (Figure 4). Considering that approximately 50% of tropical forest AGB is made up of carbon (MCTI, Ministério da Ciência, Tecnologia e Inovação, 2020), we found that a complete restoration cycle from bare soil to dense forest would involve around 74.52 tons of carbon per hectare being stored in the aboveground layer. Such carbon sequestration gathers

$4.67 \text{ t C ha}^{-1}$  (90% PI [1.62–13.48]) from the establishment of RF, plus  $10.89 \text{ t C ha}^{-1}$  (90% PI [3.77–31.47]) as PW becomes established. The majority of C is stored as PW transition to DF, with another  $58.96 \text{ t C ha}^{-1}$  (90% PI [20.41–170.34]) sequestered. This is the latest secondary stage we have considered.

## AGB estimation across the study region

Vegetation classification of high-resolution recent satellite images in 61,616 points randomly distributed along the study region inside the 83 sampling land units showed similar amounts of noncultivated terrestrial areas in sugarcane-dominated (=11.4%; SD = 5.1%) and eucalyptus-dominated areas (=11.6%; SD = 7.7%). These percentages exclude aquatic environments such as wetlands and reservoirs, which were found to cover 6.1% of sampled areas. At this first branching level, which separates human land uses and natural/seminatural cover, our results corroborated the MapBiomass, 2022 classification for 93.9% of the samples. Our classification resulted in further branching of natural/seminatural cover in three degradation stages (RF, PW, and DF). PW was found to be the most abundant class, covering 5.6% of sugarcane-dominated areas and 4.6% of eucalyptus-dominated areas. The context of sugarcane fields was associated with a lower abundance of DF (2.5%) and a slightly higher abundance of RF (3.3%) compared with the context of eucalyptus forestry with average covers of 4.0% for DF and 3.1% for RF (Figure 5).

After multiplying the dominance of degradation stages by the respective AGB average measured in the reference land units, we could investigate factors influencing the AGB distribution. Then, against our expectations, agricultural type did not substantially affect the amount of AGB in sampling land units: sugarcane-dominated areas showed an average of  $4.77 \text{ t ha}^{-1}$  (between  $Q_{25} = 2.15$  and  $Q_{75} = 8.74$ ), while for eucalyptus-dominated areas the mean value was  $4.96 \text{ t ha}^{-1}$  (between  $Q_{25} = 1.84$  and  $Q_{75} = 11.23$ ). Also, we did not find greater AGB in regeneration fragments surrounded by younger land uses: land units where the last agricultural use conversion took place less than 20 years ago showed average AGB of  $4.96 \text{ t ha}^{-1}$  (between  $Q_{25} = 2.2$  and  $Q_{75} = 8.71$ ), whilst mosaics converted more than 20 years ago had mean AGB of  $4.71 \text{ t ha}^{-1}$  (between  $Q_{25} = 1.83$  and  $Q_{75} = 11.36$ ). When testing agricultural type (sugarcane or eucalyptus), age of current agricultural use, and the interaction between agricultural type and age as predictors of regenerating biomass in sampled mosaics, none of the tested predictors (in  $\text{AGB} \sim \text{type} + \text{age} + \text{type} : \text{age} \mid \text{physiognomy} + \text{ecoregion}$ ) had a significant



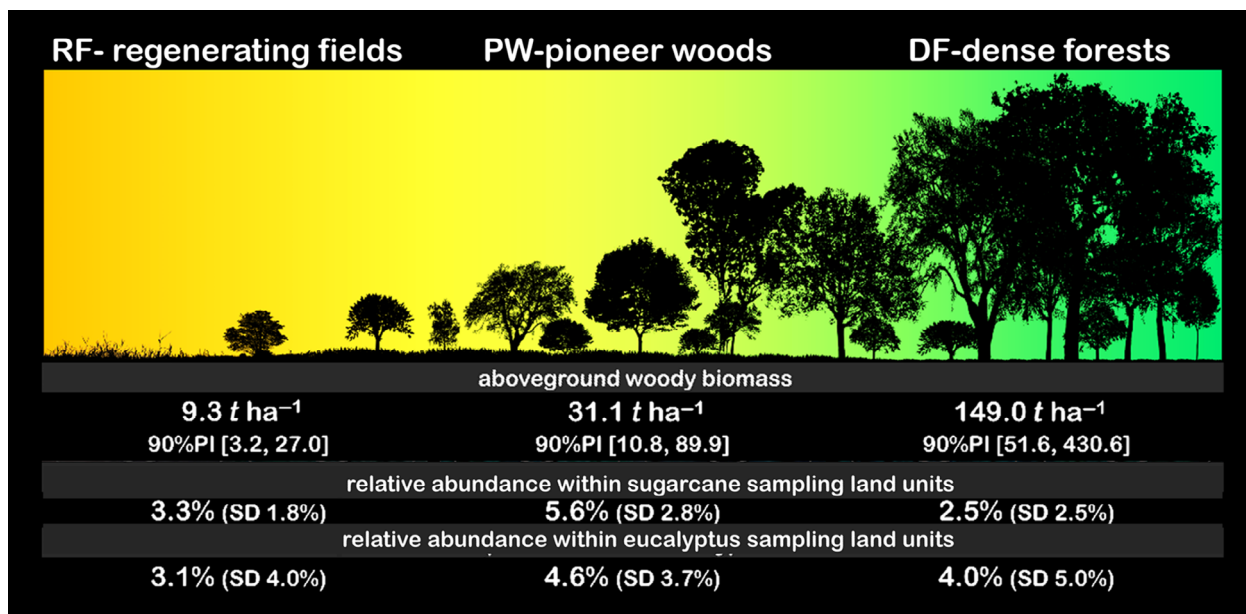


**FIGURE 4** Graphical representation of the three degradation classes: regeneration fields, pioneer woodland, and dense forests. The table in the bottom relates these classes with aboveground biomass model predictions and intervals, and relative abundances found with sampling land units in sugarcane-dominated areas and in eucalyptus-dominated areas.

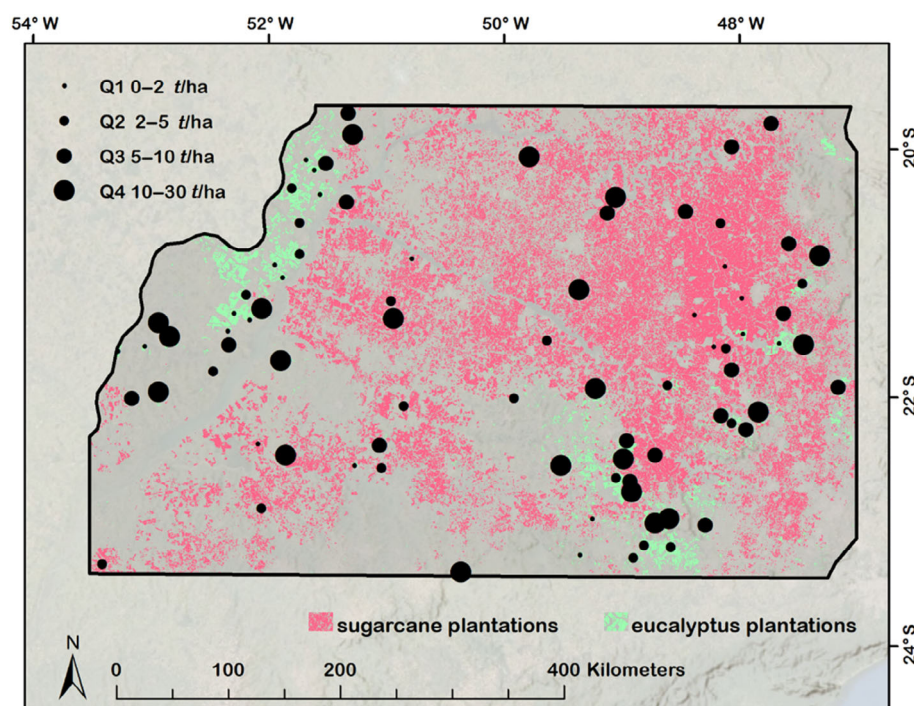


**FIGURE 5** Spatial distribution of sampling land units within the study region. Landscape scale aboveground biomass (AGB) estimates are presented in quartiles of AGB per hectare of agricultural mosaic, showing the lack of spatial tendency.

effect on AGB, (ANOVA  $p$ -values of 0.7850 for agricultural type, 0.8534 for the age of the agricultural use, and 0.0793 for the interaction between type and age). Marginal and conditional determination coefficients were low and similar for this model (i.e.,  $R_m^2 = 0.038$  and  $R_c^2 = 0.045$ ),

indicating that AGB variation was poorly explained by fixed and random factors.

Forest cover measured in the sampling land units showed significant clustering (Moran's Index: 0.1443,  $p$ -value: 0.0001), which was weakened by degradation



stochasticity resulting in the marginally random spatial distribution of AGB (Moran's Index: 0.0614,  $p$ -value: 0.0700). Therefore, our results do not suggest the presence of AGB hotspots or any cold spot in the study region (Figure 6). Consistently, our results did not support a strong effect of the ecoregion and historic vegetation domains, which were tested as random effects; neither of agricultural type, which was tested as a fixed effect and showed clear spatial clustering.

As spatial autocorrelation is not an important factor for our AGB projections, and agriculture type and age are not useful as additional predictors, we investigated the simple linear regression of AGB as a function of the mapped area covered by forest. Using forest cover data provided by the MapBiomass platform (standard 30 m LANDSAT resolution) and the degradation we assessed through very high-resolution imagery (i.e., AGB projected abundances of degradation classes [RF, PW and DF] divided by an optimal AGB in which the entire fragment is considered as DF), we confirmed that forest cover ratio and forest degradation are good predictors of forest AGB, and also that forest cover ratio is not correlated with the observed degradation of forests. Alone, forest cover quantified with raw MapBiomass data explained 73% of AGB variation (Figure 7a), while degradation (observed AGB: optimal AGB) explained 61% of AGB variation (Figure 7b). The association between these factors was surprisingly low ( $R^2 = 0.24$ , besides an ANOVA  $p$ -value  $< 0.001$ ) (Figure 7c).

Our results corroborate forest cover as an effective predictor of AGB. Nevertheless, we evidenced a crucial caveat: huge AGB overestimation emerges if forest degradation is not accounted for, because there is a

considerable loss of AGB by degradation. Thus, in areas where we did not observe anthropic land use the average AGB was  $54.98 \text{ t ha}^{-1}$ . Even in areas mapped by MapBiomass (2022) as forested, the average AGB was  $79.52 \text{ t ha}^{-1}$ , nearly half of the  $149.04 \text{ t ha}^{-1}$  we found as the average for secondary forests. Furthermore, the simplest linear model of AGB as a function of mapped forest cover required a log transformation of AGB and a square root transformation of forest cover, and projected an “AGB:forest cover” relationship far below our idealized  $1.49 \text{ t ha}^{-1}$  for each 1% of forest cover {i.e.,  $5.85 \text{ t ha}^{-1}$  (90% PI = [2.25, 12.06])  $\text{t ha}^{-1}$  for the 7.36% average forest cover of sugarcane samples, and  $6.56 \text{ t ha}^{-1}$  (90% PI = [2.63, 13.21])  $\text{t ha}^{-1}$  for the 8.19% average forest cover of eucalyptus samples; Figure 7}.

### AGB estimation context—baselines for projections

In a study area delineated to include highly agricultural territories, only 0.8% of the forest cover was found within the urban context and 31.2% were grouped within natural matrices (i.e., mostly forests, with rare wetlands and grasslands). Urban-dominated areas comprised 2.9% and predominantly-natural areas comprised 6.5% of our study region. Conversely, 90.6% of our study region, is mainly covered by agriculture (i.e., agriculture is the dominant land cover at a 1-km<sup>2</sup> resolution), comprising 68.0% of the natural forests mapped in our study region. In this case, we found an average forest cover of 8.2%, and this fraction is the focus of our study. More strictly, sugarcane and eucalyptus are the predominant land uses

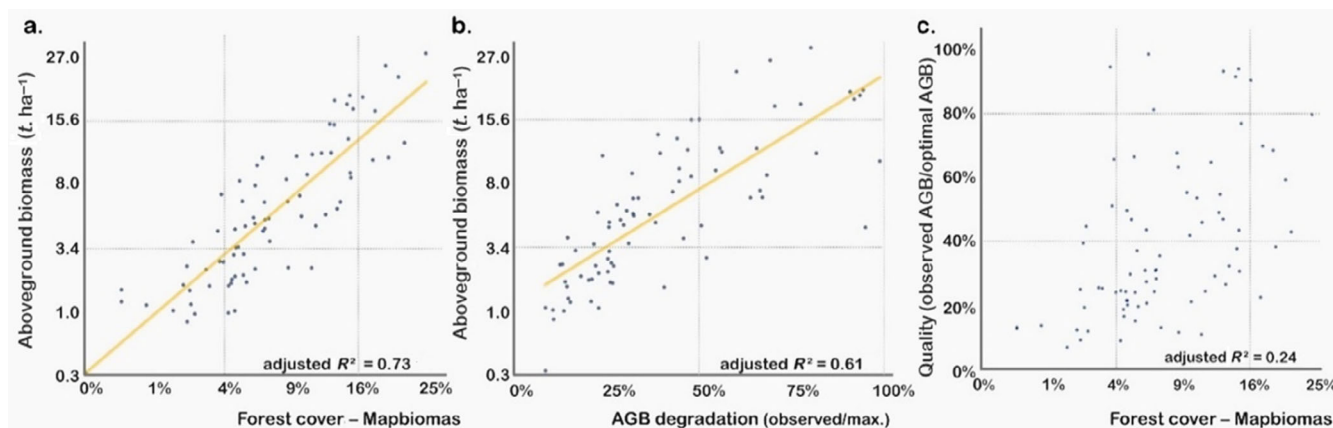


**FIGURE 6** Patterns found with sampling land units: (a) aboveground biomass (AGB) as a function of conventional forest cover. In this case, residuals are basically driven by environmental degradation. Thus, upper limits show AGB at low degradation; (b) AGB as a function of degradation; (c) Poor correlation between fragment quality (observed AGB divided by predicted AGB if dense forest). In spite of the heavy degradation found in areas with extremely low forest cover, the quality of fragments was highly variable in the sampling land units intermediately and highly forested.

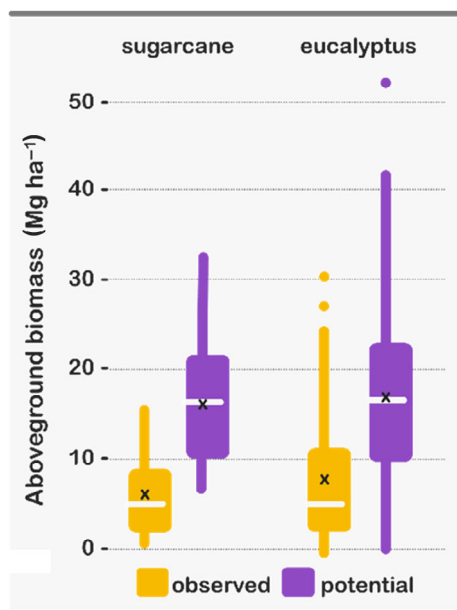


**FIGURE 7** Difference between observed and potential aboveground biomass (AGB) for sugarcane and eucalyptus mosaics, showing similar values for both land uses. The potential AGB considers all fragments as dense forests.

in, respectively, 37.0% and 3.9% of the study region, and together they host 28.6% of the study region's forests.

## DISCUSSION

Our vegetation classification based on vegetation quality, as indicated by crown cover and crown size, allowed AGB prediction without the need to control for land use, at least for the two land uses considered here. Transferring these relationships to the entire study region, our land units showed very variable seminatural AGB (between  $Q_{25} = 2.15 \text{ t ha}^{-1}$  and  $Q_{75} = 8.74 \text{ t ha}^{-1}$  in sugarcane plantations; between  $Q_{25} = 1.84 \text{ t ha}^{-1}$  and  $Q_{75} = 11.23 \text{ t ha}^{-1}$  in eucalyptus plantations), which was unaffected by land-use type and age. On average, the AGB we observed in these landscapes is less than 5% of the  $149.04 \text{ t ha}^{-1}$  we found in dense secondary forests. Most importantly, we found that such figures of massive AGB loss are indeed related to the loss of forested area, and also highly correlated with forest degradation. Hence, classifying seminatural vegetation according to degradation stages and translating results into AGB provided the opportunity to improve general expectations on the scarcity of resources required by wildlife in tropical agricultural ecosystems.

Our results show that in agricultural landscapes, the extent of forest land cover is a vague and biased indicator of trophic resources. Following the Marrakech Accords of

the Kyoto Protocol (UNFCCC, United Nations Framework Convention on Climate Change Secretariat, 2002), Brazil adopted a very inclusive definition for forests: at least 30% cover by trees at least 5 m tall at maturity (MCTI, Ministério da Ciência, Tecnologia e Inovação, 2020). Transferring such definition to this study, all the DFs and PWs are classified as forests, as well as the woodiest RFs, which according to our results show a very wide AGB range—between 30 and  $430 \text{ t ha}^{-1}$ —and the size of this interval indicates how limited is forest land cover as an indicator of the carrying capacity for wildlife. Furthermore, forest cover tends to support a biased picture because forest degradation results in disproportionately low AGB stocks inside the fragments. For instance, the average AGB we found in areas mapped as forest by MapBiomass (2022) was only  $79.52 \text{ t ha}^{-1}$ , which is far below the  $149.0 \text{ t ha}^{-1}$  we found within areas we classified as DF. In other words, the loss of 90% of forest cover does not mean that 10% of AGB is kept, as nearly half of it is missing due to degradation.

We observed relevant limitations in the correlation between forest cover and AGB, and this suggests reflection on the application of ecological thresholds for human-altered areas. For instance, it has been supported that around 30% of forest cover is required to prevent the local extinction of nongeneralist tropical forest species (e.g., Arroyo-Rodríguez et al., 2020; Banks-Leite et al., 2014). The average forest cover in our sampling land units was 7.4%, indicating a critical condition. Interestingly, if it would be possible to quadruple the lands spared by agriculture in our study region (from the current 10.8% to 43.1% of land) and keep the current degradation standards, forest cover and “natural” AGB would be quadrupled to 29.8% and  $23.7 \text{ t ha}^{-1}$ , respectively. Conversely, if protected areas were doubled and restored, reaching 21.5% of forest cover, we could expect a “natural” AGB of  $27.1 \text{ t ha}^{-1}$ . Farmers would definitely prefer the second scenario, and possibly that would also be better for forest-dwelling species due to a lesser AGB dilution. Therefore, land-use policies for conservation may be greatly improved by including the dimension of degradation, which could be quite easily reflected in the quantification of biomass. Still, the comparison of these two scenarios must consider that legal compliance would be fully achieved in our study region, around 25% of protection (Legal Reserves, RL + permanent protection areas, APP; determined by the LPVN; see d’Albertas et al., 2023).

Our study indicates that the agricultural mosaic should be more than 20 times larger than a preserved forest to host the same amount of native AGB (1:20 AGB dilution). Thus, the present condition of native biomass scarcity suggests supporting generalist species able to move through long distances, including crossing-matrix dispersal (i.e., biological fluxes through agricultural fields

or commercial forests), and expectations of massive loss of forest-specialist taxa at highly deforested tropical landscapes (e.g., Pardini et al., 2010) is fully applicable to our study region. Nevertheless, there is evidence of a possible increase in carnivore abundance in both savannas (Baylis, 1987) and forest patch groups at higher degradation (Shachak et al., 2008). Future studies should prioritize how different biological groups respond to forest degradation in agricultural landscapes to improve their biodiversity monitoring (Verdade et al., 2014).

Our models showed the low importance of the effect of agricultural type and age on forest quality as indicated by AGB and, thus, we did not include these factors in AGB projections. Possibly, the time scale was fundamental in rejecting these predictors of AGB. Widespread forest degradation caused by an intensification of human-induced disturbance, as highlighted by Barlow et al. (2016) and Silva-Junior, Aragão, et al. (2020), possibly occurred before 1985, that is the limit date of our land-use dataset (MapBiomass, 2022). Also, the disturbance history of the studied fragments is variable and, at the current stage, a considerable portion of fragments may suffer recurrent human changes directly promoted by human activities, as reported by Piffer et al. (2022), rather than a continuous forest degradation driven by externalities of adjacent land use. Conversely, it is possible that fragments are still reflecting past land uses (predominantly pastures), which were different from the present uses and in the future will reflect different trajectories consistent with the current land uses (Arroyo-Rodríguez et al., 2020; Verdade et al., 2014, 2016). Nevertheless, similar results for such distinct agricultural uses suggest that the patterns we found are likely transferable to other agricultural uses.

We note that using forest degradation categories is not recommended when more direct approaches are available to quantify AGB, as we did with our reference land units, and as possible with other alternatives requiring specific aerial surveying (e.g., d'Oliveira et al., 2020; Wang et al., 2023). By focusing on categories clearly detectable by the human eye and easily trained when using machine learning, we introduce a step that treats a continuous variable in a discrete manner. Separating PW, RF, and DF involves imposing artificial boundaries for continuous forest degradation or regeneration conditions. Furthermore, from this perspective, such cut-offs may be as arbitrary as those customarily used for the forested-deforested dichotomy. Nevertheless, PW-RF-DF categorization relates to AGB magnitudes in a helpful manner for conservation. For example, in our study region, we observed that the AGB of PW tends to be three times higher than in regenerating fields but five times lower than in DF. These proportions illustrate how rewarding it

can be to assist secondary growth in pioneer fields and woods.

AGB monitoring could also support compensatory measures (see de Mello et al., 2021) as a means of comparing fragments with different forest quality settings. Opportunely, AGB monitoring would also directly address the climate agenda. Our study region comprises 1.22 million ha of seminatural fragments and corridors embedded in sugarcane and eucalyptus plantations, where we observed an average AGB deficit of  $94.06 \text{ t ha}^{-1}$  compared with DF. Therefore, a successful forest restoration of these lands already spared by agriculture would involve an AGB increase of 114.75 million tons, which, according to coefficients from an extensive literature review organized by the Brazilian carbon emissions report (MCTI, Ministério da Ciência, Tecnologia e Inovação, 2020), is equivalent to 284.6 million tons of  $\text{CO}_2$ . Based on the compilation of hundreds of scientific studies, this governmental synthesis indicates that (1) AGB gathers 73.92% of the total forest carbon (excluding soil) in our study region while another 26.08% is stored in roots and litter; (2) approximately 50% of the AGB of tropical forests is made up of carbon, therefore, the biomass deficit in current fragments of the study area involves 77.62 million tons of carbon, which is equivalent to the mentioned 284.60 million tons of  $\text{CO}_2$ . This is a considerable amount that represents 25% of the Brazilian target annual emission by 2030 under the Paris Agreement, which has been undermined by current Brazilian forest policies (Silva-Junior et al., 2021). Furthermore, considering that the forest sequestrations of  $\text{CO}_2$  equivalent have been negotiated above US\$15/ton in the voluntary carbon market, repairing this AGB deficiency involves around US\$4.27 billion. The magnitude of such financial resource is undoubtedly relevant if compared with the US\$23.5 billion estimated as the annual agricultural production of São Paulo state, of which US\$7.6 billion are attributed to sugarcane (IEA, 2020). These figures support that large-scale forest restoration efforts are economically feasible. An increase in forest cover consistent with Brazilian legal requirements combined with maximizing forest quality would at least quadruple natural AGB, and in consequence, the trophic resources that support wildlife.

## CONCLUSIONS

This research suggests the benefits of adopting natural/seminatural AGB as an indicator of wildlife support in agricultural landscapes within tropical forest ecoregions. The proposed remotely sensed AGB assessment was



proven fully accessible and should guide future wildlife management as well as agriculture/silvicultural certification processes. Also, it can be implemented with machine learning techniques enabling large-scale monitoring. Our case study illustrates a tropical agricultural conversion reaching 90% of land occupation. At this point, one-third of forests were grouped in small regions of minor farming, while the other two-thirds were scattered in small patches and narrow corridors embedded in farmland. At very high resolution, we observed that these fragments conventionally mapped as forests are actually successional mosaics predominantly covered by early regeneration. Degradation nearly halves AGB in areas spared by agriculture, which combined with deforestation and land-use conversion, reduces seminatural AGB by 95% at the landscape scale. Consequently, most of the land being destined for protection is neither farmed nor conserved, and this pattern likely persists for decades. So far, restricting land use has not been enough to ensure minimal resources for wildlife populations, and further efforts must be employed in ecological restoration before areas destined for protection and mapped as natural habitat fragments are accountable as functional pieces of natural systems.

## ACKNOWLEDGMENTS

The authors gratefully acknowledge the financial support from the FAPESP-São Paulo Research Foundation (Procs. Nos. 17/01304-4, 21/00044-4 and 20/10238-8) and the CNPq-Brazilian Council for Scientific and Technological Development (Proc. No. 304559/2021). We would like to thank Dr. Xiangming Xiao and anonymous reviewers for their constructive feedback that substantially improved the manuscript.

## CONFLICT OF INTEREST STATEMENT

The authors declare no conflicts of interest.

## DATA AVAILABILITY STATEMENT

Data and code (Toledo et al., 2023) are available in Figshare at <https://doi.org/10.6084/m9.figshare.21920679>.

## ORCID

Renato Miazaki de Toledo  <https://orcid.org/0000-0002-0152-2797>

Michael Philip Perring  <https://orcid.org/0000-0001-8553-4893>

## REFERENCES

- Almeida, C. T., L. S. Galvão, L. E. d. O. C. e. Aragão, J. P. H. B. Ometto, A. D. Jacon, F. R. d. S. Pereira, L. Y. Sato, et al. 2019. "Combining LiDAR and Hyperspectral Data for Aboveground Biomass Modelling in the Brazilian Amazon Using Different Regression Algorithms." *Remote Sensing of Environment* 232: 111323.
- APG—Angiosperm Phylogeny Group, M. W. Chase, M. J. M. Christenhusz, M. F. Fay, J. W. Byng, W. S. Judd, D. E. Soltis, et al. 2016. "An Update of the Angiosperm Phylogeny Group Classification for the Orders and Families of Flowering Plants: APG IV." *Botanical Journal of the Linnean Society* 181(1): 1–20.
- Arroyo-Rodríguez, V., L. Fahrig, M. Tabarelli, J. I. Watling, L. Tischendorf, M. Benchimol, E. Cazetta, et al. 2020. "Designing Optimal Human-Modified Landscapes for Forest Biodiversity Conservation." *Ecology Letters* 23(9): 1404–20.
- Banks-Leite, C., R. Pardini, L. R. Tambosi, W. D. Pearse, A. A. Bueno, R. T. Bruscagin, T. H. Condez, et al. 2014. "Using Ecological Thresholds to Evaluate the Costs and Benefits of Set-Asides in a Biodiversity Hotspot." *Science* 345(6200): 1041–45.
- Barlow, J., G. D. Lennox, J. Ferreira, E. Berenguer, A. C. Lees, R. M. Nally, J. R. Thomson, et al. 2016. "Anthropogenic Disturbance in Tropical Forests Can Double Biodiversity Loss from Deforestation." *Nature* 535(7610): 144–47.
- Bastin, J.-F., E. Rutishauser, J. R. Kellner, S. Saatchi, R. Pélissier, B. Hérault, F. Slik, et al. 2018. "Pan-Tropical Prediction of Forest Structure from the Largest Trees." *Global Ecology and Biogeography* 27(11): 1366–83.
- Baylis, P. 1987. "Kangaroo Dynamics." In *Kangaroos: Their Ecology and Management in the Sheep Rangelands of Australia*, edited by G. Caughley, N. Shepherd, and J. Short, 119–134. Sydney, NSW: Cambridge University Press.
- Chave, J., D. Coomes, S. Jansen, S. L. Lewis, N. G. Swenson, and A. E. Zanne. 2009. "Towards a Worldwide Wood Economics Spectrum." *Ecology Letters* 12(4): 351–366.
- Chave, J., M. Réjou-Méchain, A. Búrquez, E. Chidumayo, M. S. Colgan, W. B. C. Delitti, A. Duque, et al. 2014. "Improved Allometric Models to Estimate the Aboveground Biomass of Tropical Trees." *Global Change Biology* 20(10): 3177–90.
- d'Albertas, F., P. Ruggiero, L. F. G. Pinto, G. Sparovek, and J. P. Metzger. 2023. "Agricultural Certification as a Complementary Tool for Environmental Law Compliance." *Biological Conservation* 277: 109847.
- de Almeida, D. R. A., S. C. Stark, R. Valbuena, E. N. Broadbent, T. S. F. Silva, A. F. de Resende, M. P. Ferreira, et al. 2020. "A New Era in Forest Restoration Monitoring." *Restoration Ecology* 28(1): 8–11.
- de Mello, K., A. N. Fendrich, C. Borges-Matos, A. D. Brites, P. A. Tavares, G. C. da Rocha, M. Matsumoto, et al. 2021. "Integrating Ecological Equivalence for Native Vegetation Compensation: A Methodological Approach." *Land Use Policy* 108: 105568.
- Dias, L. C. P., F. M. Pimenta, A. B. Santos, M. H. Costa, and R. J. Ladle. 2016. "Patterns of Land Use, Extensification, and Intensification of Brazilian Agriculture." *Global Change Biology* 22(8): 2887–2903.
- Dinerstein, E., D. Olson, A. Joshi, C. Vynne, N. D. Burgess, E. Wikramanayake, N. Hahn, et al. 2017. "An Ecoregion-Based Approach to Protecting half the Terrestrial Realm." *Bioscience* 67(6): 534–545.
- d'Oliveira, M. V. N., E. N. Broadbent, L. C. Oliveira, D. R. A. Almeida, D. A. Papa, M. E. Ferreira, A. M. Almeyda

- Zambrano, et al. 2020. "Aboveground Biomass Estimation in Amazonian Tropical Forests: A Comparison of Aircraft-and Gatoreye UAV-Borne LIDAR Data in the Chico Mendes Extractive Reserve in Acre, Brazil." *Remote Sensing* 12(11): 1754.
- Dudley, N., and S. Alexander. 2017. "Agriculture and Biodiversity: A Review." *Biodiversity* 18(2–3): 45–49.
- Duncanson, L., J. Armston, M. Disney, V. Avitabile, N. Barbier, K. Calders, S. Carter, et al. 2019. "The Importance of Consistent Global Forest Aboveground Biomass Product Validation." *Surveys in Geophysics* 40(4): 979–999.
- ESRI. 2020. *ArcGIS Desktop: Release 10.6*. Redlands, CA: Environmental Systems Research Institute.
- FAO. 2020. *World Food and Agriculture Statistical Yearbook 2020*. Rome: FAO. <https://doi.org/10.4060/cb1329en>.
- Hansen, M. C., L. Wang, X.-P. Song, A. Tyukavina, S. Turubanova, P. V. Potapov, and S. V. Stehman. 2020. "The Fate of Tropical Forest Fragments." *Science Advances* 6: eaax8574.
- IBGE. 2017. "Mapa de vegetação do Brasil." In *Fundação Instituto Brasileiro de Geografia e Estatística*. Rio de Janeiro: IBGE [www.ibge.gov.br/geociencias/informacoesambientais/vegetacao/22453-cartas-1-250-000.html?=&t=acesso-ao-produto](http://www.ibge.gov.br/geociencias/informacoesambientais/vegetacao/22453-cartas-1-250-000.html?=&t=acesso-ao-produto).
- IEA. 2020. *Agropecuária Paulista em 2022*. São Paulo, Brazil: Instituto de Economia Agrícola. <http://www.iea.agricultura.sp.gov.br>.
- Labrière, N., S. J. Davies, M. I. Disney, L. I. Duncanson, M. Herold, S. L. Lewis, O. L. Phillips, et al. 2022. "Toward a Forest Biomass Reference Measurement System for Remote Sensing Applications." *Global Change Biology* 29: 827–840.
- Lohbeck, M., L. Poorter, M. Martínez-Ramos, and F. Bongers. 2015. "Biomass Is the Main Driver of Changes in Ecosystem Process Rates during Tropical Forest Succession." *Ecology* 96(5): 1242–52.
- MacArthur, R. H., and E. O. Wilson. 1967. *The Theory of Island Biogeography*. Princeton, NJ: Princeton University Press.
- Mapbiomas. 2022. "Plataforma Mapbiomas Coleção 6." <https://plataforma.mapbiomas.org/>.
- MCTI—Ministério da Ciência, Tecnologia e Inovação. 2020. "Quarta Comunicação Nacional e Relatórios de Atualização Bial do Brasil à Convenção-Quadro das Nações Unidas Sobre Mudança do Clima—Relatório de Referência Setor Uso da Terra—Mudança do Uso da Terra e Florestas." <https://www.gov.br/mcti/pt-br/acompanhe-o-mcti/sirene/publicacoes/relatorios-de-referencia-setorial>.
- Myers, N., R. A. Mittermeier, C. G. Mittermeier, G. A. B. Da Fonseca, and J. Kent. 2000. "Biodiversity Hotspots for Conservation Priorities." *Nature* 403(6772): 853–58.
- Nakagawa, S., P. C. D. Johnson, and H. Schielzeth. 2017. "The Coefficient of Determination R<sup>2</sup> and Intra-Class Correlation Coefficient from Generalized Linear Mixed-Effects Models Revisited and Expanded." *Journal of the Royal Society Interface* 14(134): 20170213.
- Nobre, C. A., G. Sampaio, L. S. Borma, J. C. Castilla-Rubio, J. S. Silva, and M. Cardoso. 2016. "Land-Use and Climate Change Risks in the Amazon and the Need of a Novel Sustainable Development Paradigm." *Proceedings of the National Academy of Sciences* 113(39): 10759–68.
- Pardini, R., A. de Arruda Bueno, T. A. Gardner, P. I. Prado, and J. P. Metzger. 2010. "Beyond the Fragmentation Threshold Hypothesis: Regime Shifts in Biodiversity across Fragmented Landscapes." *PLoS One* 5(10): e13666.
- Piffer, P. R., M. R. Rosa, L. R. Tambosi, J. P. Metzger, and M. Uriarte. 2022. "Turnover Rates of Regenerated Forests Challenge Restoration Efforts in the Brazilian Atlantic Forest." *Environmental Research Letters* 17(4): 045009.
- Pimm, S. L., C. N. Jenkins, and V. L. Binbin. 2018. "How to Protect Half of Earth to Ensure it Protects Sufficient Biodiversity." *Science Advances* 4: eaat2616.
- Poorter, L., D. Craven, C. C. Jakovac, M. T. van der Sande, L. Amissah, F. Bongers, R. L. Chazdon, et al. 2021. "Multidimensional Tropical Forest Recovery." *Science* 374(6573): 1370–76.
- Potapov, P., S. Turubanova, M. C. Hansen, A. Tyukavina, V. Zalles, A. Khan, X.-P. Song, A. Pickens, Q. Shen, and J. Cortez. 2022. "Global Maps of Cropland Extent and Change Show Accelerated Cropland Expansion in the Twenty-First Century." *Nature Food* 3(1): 19–28.
- Rayden, T., K. R. Jones, K. Austin, and J. Radachowsky. 2023. "Improving Climate and Biodiversity Outcomes through Restoration of Forest Integrity." *Conservation Biology* 37: e14163.
- Satdichanh, M., H. Ma, K. Yan, G. G. O. Dossa, L. Winowiecki, T.-G. Vågen, A. Gassner, J. Xu, and R. D. Harrison. 2019. "Phylogenetic Diversity Correlated with above-Ground Biomass Production during Forest Succession: Evidence from Tropical Forests in Southeast Asia." *Journal of Ecology* 107(3): 1419–32.
- Shachak, M., B. Boeken, E. Groner, R. Kadmon, Y. Lubin, E. Meron, G. Ne'Eman, A. Perevolotsky, Y. Shkedy, and E. D. Ungar. 2008. "Woody Species as Landscape Modulators and their Effect on Biodiversity Patterns." *Bioscience* 58(3): 209–221.
- Silva-Junior, C. A., P. E. Teodoro, R. C. Delgado, L. P. R. Teodoro, M. Lima, A. de Andréa, F. H. Pantaleão, et al. 2020. "Persistent Fire Foci in all Biomes Undermine the Paris Agreement in Brazil." *Scientific Reports* 10: 1–14.
- Silva-Junior, C. H. L., L. E. O. C. Aragão, L. O. Anderson, M. G. Fonseca, Y. E. Shimabukuro, C. Vancutsem, F. Achard, et al. 2020. "Persistent Collapse of Biomass in Amazonian Forest Edges Following Deforestation Leads to Unaccounted Carbon Losses." *Science Advances* 6: eaaz8360.
- Silva-Junior, C. H. L., A. Pessoa, N. S. Carvalho, J. B. C. Reis, L. O. Anderson, and L. E. O. C. Aragão. 2021. "The Brazilian Amazon Deforestation Rate in 2020 Is the Greatest of the Decade." *Nature Ecology & Evolution* 5(2): 144–45.
- Sotirov, M., B. Pokorny, D. Kleinschmit, and P. Kanowski. 2020. "International Forest Governance and Policy: Institutional Architecture and Pathways of Influence in Global Sustainability." *Sustainability* 12(17): 7010.
- Souza Jr Carlos, M., J. Z. Shimbo, M. R. Rosa, L. L. Parente, A. A. Alencar, B. F. T. Rudorff, H. Hasenack, et al. 2020. "Reconstructing Three Decades of Land Use and Land Cover Changes in Brazilian Biomes with Landsat Archive and Earth Engine." *Remote Sensing* 12(17): 2735.
- Toledo, R., V. R. Pivello, M. Perring, and L. M. Verdade. 2023. "Natural Vegetation Biomass and the Dimension of Forest Quality in Tropical Agricultural Landscapes." Figshare, Dataset. <https://doi.org/10.6084/m9.figshare.21920679.v2>.
- Toledo, R. M., R. F. Santos, K. Verheyen, and M. P. Perring. 2018. "Ecological Restoration Efforts in Tropical Rural Landscapes: Challenges and Policy Implications in a Highly Degraded Region." *Land Use Policy* 75: 486–493.

- UNEP—United Nations Environment Programme World Conservation Monitoring Centre. 2016. “Protected Planet Report 2016.” In *UNEP-WCMC and IUCN* 78–95. UK and Switzerland: Cambridge.
- UNFCCC—United Nations Framework Convention on Climate Change Secretariat. 2002. “Report of the Conference of the Parties on its Seventh Session.” In *Addendum Part Two: Action Taken by the Conference of the Parties*, Vol. I. Bonn, Germany: UNFCCC.
- Verdade, L. M., C. Gheler-Costa, and M. C. Lyra-Jorge. 2016. “The Multiple Facets of Agricultural Landscapes.” In *Biodiversity in Agricultural Landscapes of Southeastern Brazil*, edited by C. Gheler-Costa, M. C. Lyra-Jorge, and L. M. Verdade, 2–13. Berlin: De Gruyter.
- Verdade, L. M., M. C. Lyra-Jorge, and C. I. Piña. 2014. “Redirections in Conservation Biology.” In *Applied Ecology and Human Dimensions in Biological Conservation*, edited by L. M. Verdade, M. C. Lyra-Jorge, and C. I. Piña, 3–17. Heidelberg: Springer-Verlag.
- Vidal, M. M., C. Banks-Leite, L. R. Tambosi, É. Hasui, P. F. Develey, W. R. Silva, P. R. Guimaraes Jr, and J. P. Metzger. 2019. “Predicting the Non-linear Collapse of Plant–Frugivore Networks Due to Habitat Loss.” *Ecography* 42(10): 1765–76.
- Wang, G., S. Li, C. Huang, G. He, Y. Li, J. Feng, F. Tang, P. Yan, and L. Qiu. 2023. “Mapping the Spatial Distribution of Above-ground Biomass in China’s Subtropical Forests Based on UAV LiDAR Data.” *Forests* 14(8): 1560.
- Wilson, E. O. 2016. *Half-Earth: Our Planet’s Fight for Life*. New York: WW Norton & Company.
- Zanne, A. E., G. Lopez-Gonzalez, D. A. Coomes, J. Ilic, S. Jansen, S. L. Lewis, R. B. Miller, N. G. Swenson, M. C. Wiemann, and J. Chave. 2009. “Global Eood Density Database.” Dryad. Identifier: <http://datadryad.org/handle/10255/dryad.235>.
- Zonneveld, I. S. 1989. “The Land Unit—A Fundamental Concept in Landscape Ecology, and its Applications.” *Landscape Ecology* 3(2): 67–86.

## SUPPORTING INFORMATION

Additional supporting information can be found online in the Supporting Information section at the end of this article.

**How to cite this article:** de Toledo, Renato Miazaki, Vania Regina Pivello, Michael Philip Perring, and Luciano Martins Verdade. 2024. “Natural Vegetation Biomass and the Dimension of Forest Quality in Tropical Agricultural Landscapes.” *Ecological Applications* 34(3): e2950. <https://doi.org/10.1002/eap.2950>